ACS OMEGA

http://pubs.acs.org/journal/acsodf

Article

Novel Short Process for *p*-Xylene Production Based on the Selectivity Intensification of Toluene Methylation with Methanol

Dongliang Wang,[‖] Junqiang Zhang,[‖] Peng Dong, Guixian Li,* Xueying Fan, and Yong Yang*

Cite This: *ACS Omega* 2022, 7, 1211−1222

Read Online

ACCESS | Metrics & More | Article Recommendations | Supporting Information

ABSTRACT: Toluene methylation using methanol offers a high potential molecular engineering process to produce *p*-xylene (PX) based on shape-selective catalysts. To further improve the process economics, a novel short process was proposed by reducing the high-energy consumption separation of xylene isomers in existing processes since the PX selectivity of the xylene isomers can be enhanced more than the industrial product quality of 99.7%. The PX selectivity intensification was achieved as a result of decreased contact time by considering factors such as the feed ratio, diluents, temperature, and pressure in a toluene methylation reactor. This proposed short process indicated that the reactor effluent could be purified only through the two conventional distillation towers by removing the methanol recovery and separation of xylene isomers. The raw material utilization, energy consumption, and economic data were also analyzed for the six contrastive cases. The short process using catalyst Si−Mg−P−La/ZSM-5 exhibited the highest effective utilization rates of 96.27 and 95.50% for toluene and methanol, respectively. The short process also showed a good economic value in terms of capital investment and operating costs due to the multistage reactor without benzene byproducts. Thus, the obtained total annual cost (TAC) value of 13 848.1 k$·year^{-1} was 68.9 and 87.9% of the two existing processes.

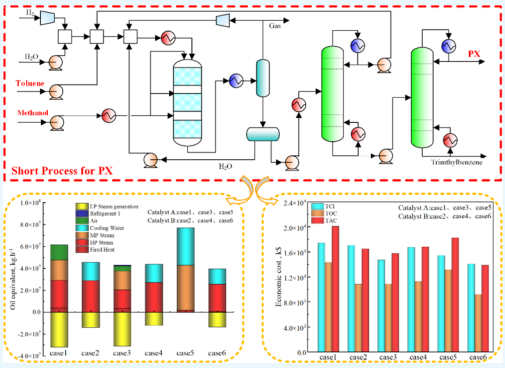

1. INTRODUCTION

p-Xylene (PX) is an important intermediate for the polyester, pharmaceutical, chemical fiber, and pesticide industries with an annual global market compound growth rate of 12.05% between 2016 and 2022.[1,2] PX is mainly produced via aromatic extraction, toluene disproportionation, C8 aromatic isomerization, and transalkylation of heavy aromatics.[3−5] These methods are typically accompanied by adsorptive separation, crystallization, and reactive distillation technologies for C8 isomers with relatively low *m*-xylene (MX) and *o*-xylene (OX) values. These separation technologies require more energy and expensive raw materials, which increases the production costs due to very similar boiling points of xylene isomers, low PX selectivity, and the considerable amount of byproducts that are produced.[3,6] Correspondingly, toluene methylation with methanol offers a potential molecular engineering process for the production of PX, based on shape-selective catalysts.[1,7−9]

To improve the advantage and competitiveness of toluene methylation, methanol has to be inexpensive and the PX selectivity in xylene isomers should be above 90.0%.[10,11] Fortunately, shape-selective zeolite catalysts provide considerable PX selectivity by improving mass transfer and covering the external acid sites.[12−14] Janardhan et al.[15] found that PX selectivity increased from 30.7 to 97.0% when the pore volume decreased from 0.30 to 0.24 cm^3/g for P-modified zeolites. However, the selectivity decreased from 97.0 to 87.0% when the pore volume further reduced from 0.20 to 0.18 cm^3/g. Kaeding et al.[16] modified an HZSM-5 molecular sieve with 8.5 wt % H_3PO_4, which was then heated at 600 °C to obtain PX with a selectivity of 97.0%. Ghiaci et al.[17] reduced the phosphorus loading to 2.1%, with a PX selectivity reaching 100%. Wang et al.[18] reported that inverse Al-zoned HZSM-5 with sinusoidal channels could maximize PX selectivity, with good activity and stability (>220 h). By covering most of the straight channels with intergrowth crystals and only exposing the zig-zag channels in HZSM-5 to external surfaces, the researchers obtained PX with a selectivity greater than 99.0%. The silicalite-1 coated Zn/ZSM-5 catalyst showed considerable catalytic performance during methanol to aromatics processing, and PX selectivity in xylene reached 99.0%.[19] Li et al.[20] reported two shape-selective HZSM-5 catalysts with similar pore sizes, which were prepared with a silicalite-1 coating or boron modification, and both exhibited a high p-xylene selectivity of over 98.0%. Moreover, other than complete methanol conversion from experimental work,[19,21] Breen et al.[11] achieved nearly 100% PX selectivity by operating catalyzed toluene gas-phase methylation at a high

Received: October 17, 2021
Accepted: December 22, 2021
Published: December 30, 2021

space velocity, using a Mg-ZSM-5 catalyst. Fan et al.[22] reported that an increase in temperature and a higher feed molar ratio of toluene to methanol could improve the main reaction rate and suppress the competitiveness of the methanol autocatalytic reaction.

However, the design process for toluene methylation, PX selectivity, product composition, and catalyst stability are the main factors that restrict the economics of this technical process. To reduce the separation cost and create a competitive toluene methylation approach for PX production, Ashraf et al.[23] developed a catalytic methylation process using a Mg-ZSM-5 catalyst, followed by reactive distillation to separate the xylene isomers. Using the built-in optimization tool in Aspen Plus, the optimized reactor parameters were set to a maximum PX selectivity of 97.7%, with an objective of 99.7 wt % for PX. The researchers found that reactive distillation reduced the energy and separation cost more than conventional separation techniques, such as crystallization or adsorption. To remove the methanol recovery and recycling systems and reduce toluene losses during downstream separation, Liu et al.[6] proposed an intensified PX production process, where the methanol conversion rate increased from 70.0 to 98.0% and PX selectivity decreased to 92.0%. Thus, this methylation technology still needs the high-energy consumption separation of xylene isomers even with the PX selectivity as high as 90−98% for the methylation process with shape-selective catalysts.

To further improve the process economics for PX production, this paper first analyzed the selectivity intensification factors to discuss the strategy of 99.7% PX selectivity for a toluene methylation reactor based on two catalytic reaction kinetics[23−25] with the idea of "Ultralow Contact Time" from ref 11. Since the 99.7% PX selectivity met a superior grade of industrial PX products, a novel short process was proposed by eliminating the high-energy unit of xylene isomer separation. Finally, the feed utilization, energy efficiency, and economic advantages for the proposed process were determined by comparing with those designed by Ashraf[23] and Liu[6] through an optimal systematic procedure and heat integration.

2. METHYLATION PROCESS AND ITS SELECTIVITY

2.1. Reaction Model for Toluene Methylation with Methanol. Researchers have conducted considerable research on toluene methylation reaction kinetics to determine the side reactions. Sotelo et al.[26] developed a kinetic model for Mg-modified catalysts in a fixed-bed reactor by considering the diffusion effects and the influence of PX isomerization over the external zeolite surface. The researchers reproduced the experimental product distribution and obtained an average relative error of 6.8%. In addition, Valverde[23,25] developed a simple power-law kinetic model for toluene alkylation with methanol using the Mg-ZSM-5 catalyst (catalyst A) and considering all possible methanol side reactions. As shown in Figure 1, the reaction system included (1) toluene methylation, (2) methanol dehydration, (3) toluene disproportionation, (4) PX dealkylation, and (5) PX isomerization. Also, as shown in Table 1, the power-law kinetics data were obtained for a temperature range of 420.0−460.0 °C.

Breen et al.[11] reported a PX selectivity close to 100% using a Mg-modified ZSM-5 catalyst at a low space-time. Tan et al.[24] also used a highly selective Si−Mg−P−La−ZSM-5 catalyst (catalyst B),[27,28] to establish a kinetics model for toluene methylation and put forward the following hypothesis. First, the toluene methanol alkylation reaction generated PX, then PX was

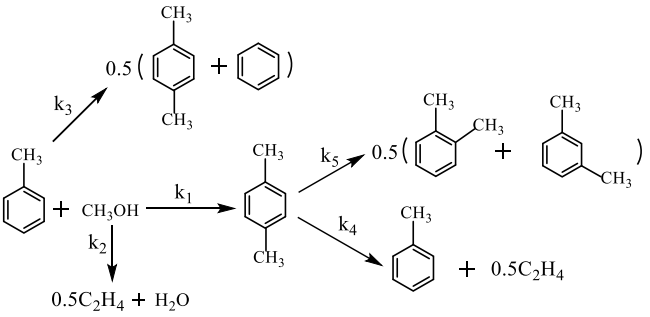

Figure 1. Reaction network of toluene alkylation with methanol.

Table 1. Reaction Kinetic and Parameters for Toluene Methylation[a]

reaction rate equation	pre-exponential factor, A_i		activation energy, E_{ai} (kJ·mol^{-1})
$r_1 = k_1 P_T P_M$	403 ± 5	mol·(g·h·atm^2)$^{-1}$	45.7 ± 0.4
$r_2 = k_2 P_M^2$	1346 ± 64	mol·(g·h·atm^2)$^{-1}$	50.6 ± 0.5
$r_3 = k_3 P_T$	96.2 ± 1	mol·(g·h·atm)$^{-1}$	59.0 ± 0.5
$r_4 = k_4 P_{PX}$	0.3815 ± 0.05	mol·(g·h·atm)$^{-1}$	19.6 ± 0.7
$r_5 = k_5 P_{PX}$	46.94 ± 0.5	mol·(g·h·atm)$^{-1}$	48.9 ± 0.3

[a]Note: r_i is the reaction rate of reaction, k_i is the rate constant, and $_{Pi}$ is the component partial pressure for component i.

isomerized into OX and MX, and PX, OX, and MX underwent deep alkylation into trimethylbenzene, with the same reaction rate constants. After reacting with the aromatics, the remaining methanol was completely dehydrated, generating olefin along with ethylene lumps. Lastly, the equilibrium constant for each reaction in the methylation system was very large, and the reverse reaction was ignored. Previous studies utilized catalyst B at temperatures of 480.0−560.0 °C with H_2O and H_2 as the carrier gases, at a total toluene methanol mass feed rate of 2.0/h.[24] Compared to catalyst A, the kinetics model for catalyst B considered the rate differences for xylene and the additional methylation of xylene. The reaction network for toluene alkylation is shown in Figure 2, and the kinetic parameters are provided in Table 2.

Using the abovementioned two kinetic models for toluene methylation, the packed bed reactor was simulated using Aspen Plus along with PR-BM as the property method. Then, the

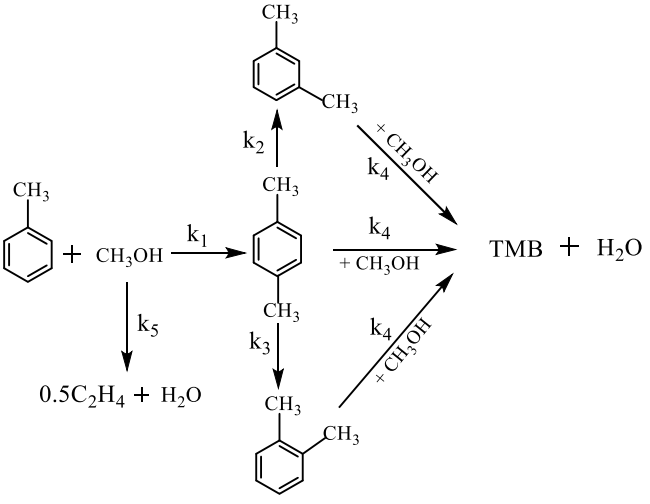

Figure 2. Reaction network of toluene alkylation with methanol.

https://doi.org/10.1021/acsomega.1c05817
ACS Omega 2022, 7, 1211−1222

Table 2. Reaction Kinetics and Parameters for Toluene Methylation[a]

reaction rate equation	pre-exponential factor, A_i		activation energy, E_{ai} (kJ·mol^{-1})
$r_1 = k_1P_TP_M$	5.66×10^5	mol·(g·h·Pa^2)$^{-1}$	76.66
$r_2 = k_2P_{PX}$	5.85×10^{-2}	mol·(g·h·Pa)$^{-1}$	19.24
$r_3 = k_3P_{PX}$	7.71×10^{-2}	mol·(g·h·Pa)$^{-1}$	16.80
$r_4 = k_4P_{PX}P_M$	1.16×10^4	mol·(g·h·Pa^2)$^{-1}$	57.47
$r_5 = k_5P_M^2$	1.73×10^4	mol·(g·h·Pa^2)$^{-1}$	44.94

[a]Note: r_i is the reaction rate of reaction, k_i is the rate constant, and $_{Pi}$ is the component partial pressure for component i.

relationships between factors such as the contact time, toluene methanol feed ratio, diluent, reaction temperature, pressure, and PX selectivity were studied.

2.2. Sensitivity Analysis for PX Selectivity. The parameters that affect toluene methylation were adjusted to achieve high PX selectivity. These factors, such as contact time, feed ratio, diluent, temperature, and pressure were introduced in the sensitivity analysis under reaction conditions of 400.0−550.0 °C, 200.0−500.0 kPa, and a toluene-to-methanol feed ratio of (F_T/F_M) = 2−8. For the sensitivity analysis, the base conditions were 300.0 kPa, F_T/F_M = 2, and space-time (W_{cat}/F_T) = 1 g·h·mol^{-1}. However, 420.0 °C was used for catalyst A and 500.0 °C for catalyst B. PX selectivity (S_{PX}) for the xylene isomers in the reaction products was defined according to the flow rates for PX, MX, and OX in the export products.

$$S_{PX} = \frac{F_{PX}^{out}}{(F_{MX}^{out} + F_{PX}^{out} + F_{OX}^{out})} \times 100\% \quad (1)$$

2.2.1. Contact Time. The ultralow contact time between the gas stream and the catalyst would result in near-perfect PX selectivity, and Breen et al.[11] achieved close to 100% PX selectivity by operating the catalyzed gas-phase methylation of toluene at a high space velocity. By adjusting the catalyst content, the contact time τ changed, and its effects on PX selectivity are shown in the ternary xylene isomer plot in Figure 3.

The S_{PX} for both catalysts increased with decreasing contact time τ. When τ was reduced to 0.2 s for catalyst A, and 0.6 s for catalyst B, S_{PX} reached 99.7%. This was attributed to the low contact time τ, which reduced the isomerization probability of the generated PX molecules on the active sites of the external catalyst.[11] However, PX had a diffusion advantage and had a diffusion coefficient 10^3−10^4 greater than MX and OX in the catalyst pores due to its smaller dynamic diameter. This made it extremely beneficial for the production of high PX selectivity at low contact times.[6,23,29,30]

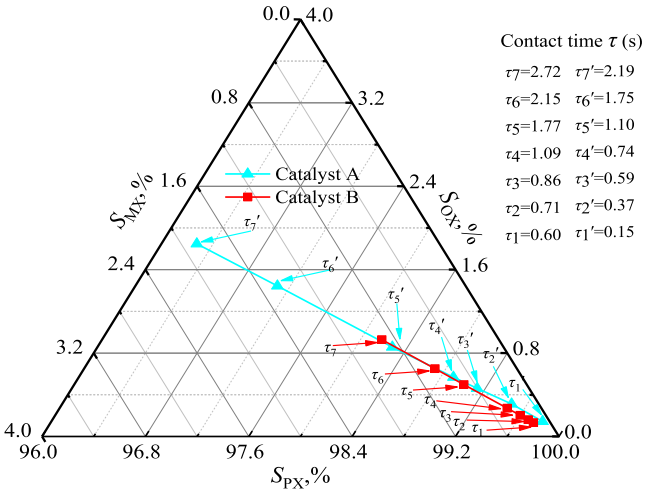

Figure 3. Ternary xylene isomer plot illustrating the effect of contact time on PX selectivity (catalyst A: at 420.0 °C, 300.0 kPa, F_T/F_M = 2.0 and catalyst B: at 500.0 °C, 300.0 kPa, F_T/F_M = 2.0).

2.2.2. Feed Ratio. The effect of toluene-to-methanol feed ratio $(m = F_T/F_M)$ on PX selectivity is shown in Figure 4, where the methanol feed rate was 500.0 kmol·h^{-1}. Once F_T/F_M increased, it indirectly enhanced the space-time W_{cat}/F_T, and S_{PX} increased accordingly. For catalyst A, S_{PX} increased from 99.0 to 99.7% when F_T/F_M increased from 2.3 to 8.0; For catalyst B, S_{PX} increased from 99.0 to 99.7% when F_T/F_M increased from 3.2 to 7.6. This indicated that the increase in F_T/F_M, not only reduced the contact time but also the PX surface concentration of the catalyst, which inhibited PX isomerization.

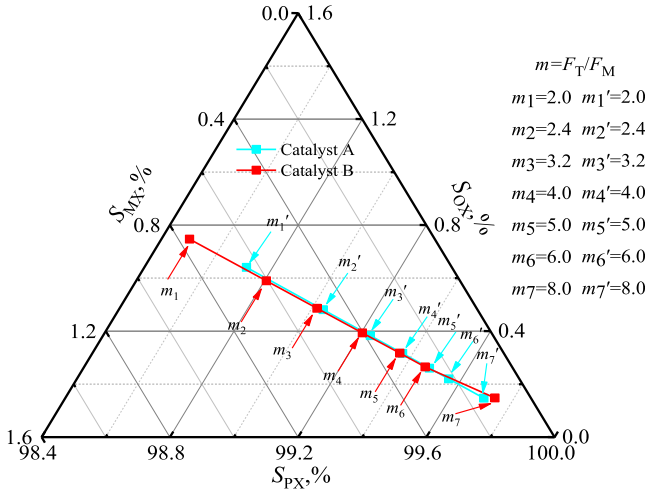

Figure 4. Effect of the toluene/methanol feed ratio on selectivity (catalyst A: at 420.0 °C, 300.0 kPa, W_{cat} = 1000.0 kg and catalyst B: at 500.0 °C, 300.0 kPa, W_{cat} = 1000.0 kg).

2.2.3. Diluents. Adding a gas-phase diluent such as hydrogen or nitrogen to the feed lowered the contact time. In addition, water played a dual role, both as a diluent and a product of the toluene methylation system. The effects of water content are shown in Figure 5, indicating that S_{PX} increased with an increase in the H_2O/methanol molar ratio (w) for both catalysts A and B. For catalyst A, S_{PX} increased from 97.1 to 99.0% and then to 99.7% when w increased from 0 to 0.3, and then to 7.4. However, for catalyst B, S_{PX} increased from 98.0 to 99.0% and then to 99.7% when w increased from 0 to 1.6 and then to 7.0. These results were consistent with the contact time, although water would inhibit the reactions as the byproducts for toluene methylation and methanol dehydration.

The effects of hydrogen or nitrogen as diluents are shown in Figure 6, showing that a high molar ratio of F_{H_2}/F_M (n) or F_{N_2}/F_M (n') intensified PX selectivity. Moreover, ethane was the only hydrogenation byproduct for ethylene derived from methanol, which prevented the system from undergoing ethyl alkylation and the catalyst from undergoing coking and carbonization. The S_{PX} reached 99.7% when n' = 7.0 for catalyst A, but n = 4.5 for catalyst B.

https://doi.org/10.1021/acsomega.1c05817
ACS Omega 2022, 7, 1211−1222

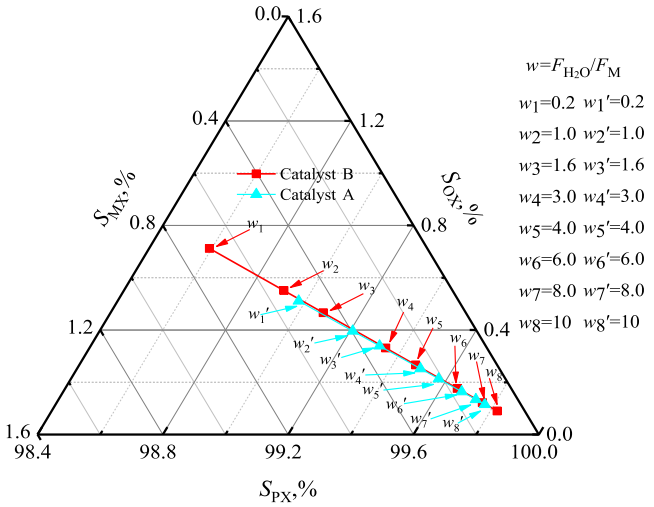

Figure 5. Effect of water amount on the selectivity (catalyst A: at 420.0 °C, 300.0 kPa, F_T/F_M = 2.0, W_{cat}/F_T =1.0 g·h·mol^{-1} and catalyst B: at 500.0 °C, 300.0 kPa, F_T/F_M = 2.0, W_{cat}/F_T = 1.0 g·h·mol^{-1}).

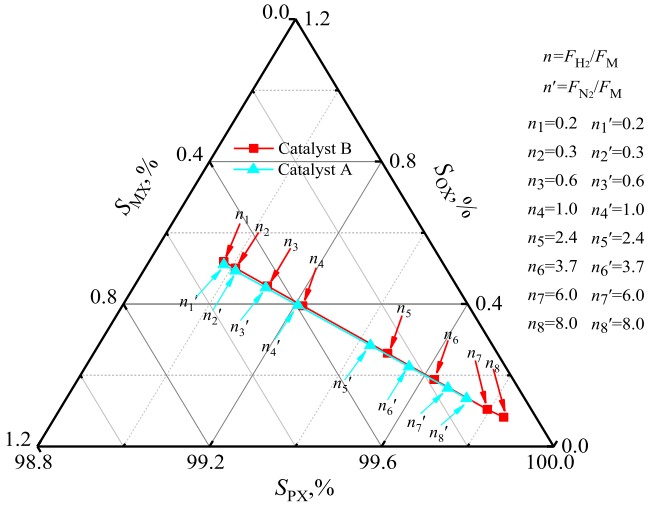

Figure 6. Effect of diluent on the selectivity (catalyst A: at 420.0 °C, 300.0 kPa, F_T/F_M = 2.0, W_{cat}/F_T =1.0 g·h·mol^{-1} and catalyst B: at 500.0 °C, 300.0 kPa, F_T/F_M = 2.0, W_{cat}/F_T =1.0 g·h·mol^{-1}).

2.2.4. Temperature. The main reactions in toluene methylation are exothermic reactions. Therefore, the reaction temperature was adjusted within 420.0−550.0 °C, and PX selectivity is plotted in Figure 7. As shown in Figure 7, S_{PX} increased from 99.0 to 99.7% for catalyst A when the reaction temperature decreased from 550.0 to 420.0 °C, and from 550.0 to 420.0 °C for catalyst B. The lower reaction temperature was more advantageous for increasing PX selectivity, as the activation energies during methylation were 45.7 and 76.6 kJ·mol^{-1}, respectively, for catalysts A and B. These values were higher than those for the PX isomerization reaction.

2.2.5. Pressure. For the kinetics reaction equation of the power exponent, the effects of reaction pressure on the reaction rate were more obvious. Figure 8 shows the effects of pressure on PX selectivity, for a range of 200.0−500.0 kPa. This showed that S_{PX} was higher than 99.7% when the pressure was reduced to 200.0 kPa for catalyst A and 270.0 kPa for catalyst B. It was speculated that pressurization was not conducive to the desorption of the preferentially generated PX, which would accelerate the isomerization reaction.[31] Therefore, a low

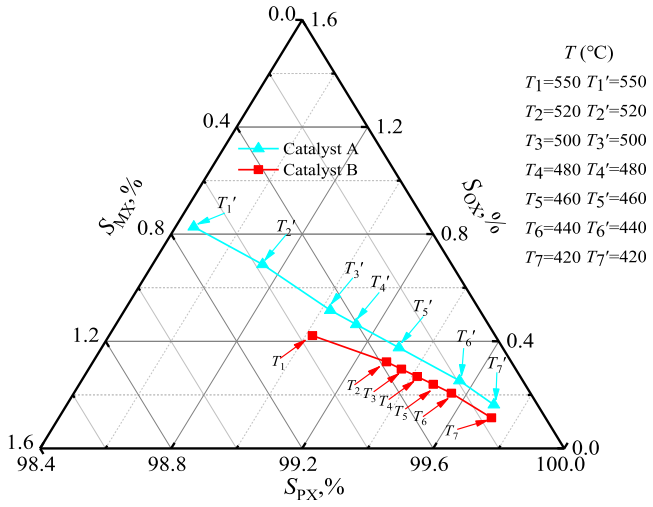

Figure 7. Effect of temperature on the selectivity (catalyst A: 300.0 kPa, F_T/F_M = 2.0, F_{H2O} = 1500.0 kmol·h^{-1}, W_{cat}/F_T = 1.0 g·h·mol^{-1} and catalyst B: 300.0 kPa, F_T/F_M = 2.00, F_{H_2O} = 1500.0 kmol·h^{-1}, W_{cat}/F_T = 1.0 g·h·mol^{-1}).

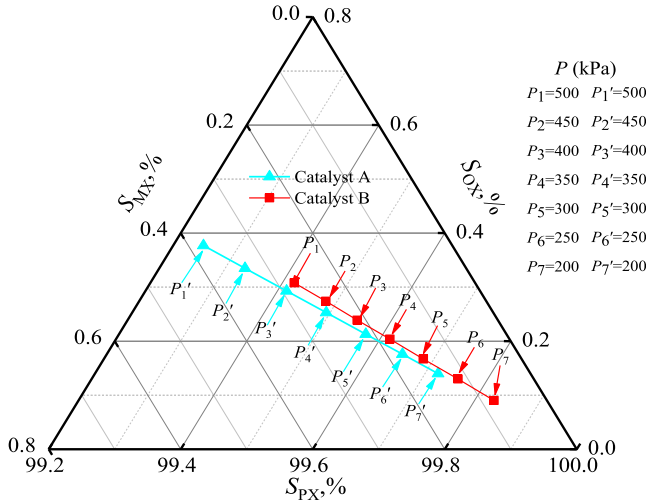

Figure 8. Effect of pressure on the selectivity (catalyst A: 420.0 °C, F_T/F_M = 2.0, W_{cat}/F_T = 1.0 g·h·mol^{-1} and catalyst B: 500.0 °C, F_T/F_M = 2.0, W_{cat}/F_T = 1.0 g·h·mol^{-1}).

reaction pressure was more conducive for improving PX selectivity.

The analysis results of the abovementioned PX selectivity influencing factors showed that the S_{PX} was more than 99.7% at a lower residence time. In addition, after gradually increasing the toluene−methanol feed ratio (F_T/F_M) and adding diluents (water, hydrogen, or nitrogen), S_{PX} significantly improved. Breen et al.[11] showed that S_{PX} was close to 100% when the toluene methylation reaction was conducted at a low altitude and using a diluent. Because the toluene−methanol feed ratio (F_T/F_M) and the diluent mainly affected the reaction space-time, this process was also a technique for modifying the space-time. In addition, when the reaction temperature and pressure increased, S_{PX} decreased accordingly. However, the conversion rate of toluene also increased. Therefore, to balance the conversion rate and PX selectivity, the selected optimized parameter ranges (reaction temperature and pressure) were 420.0−550.0 °C and 200.0−500.0 kPa.

https://doi.org/10.1021/acsomega.1c05817
ACS Omega 2022, 7, 1211−1222

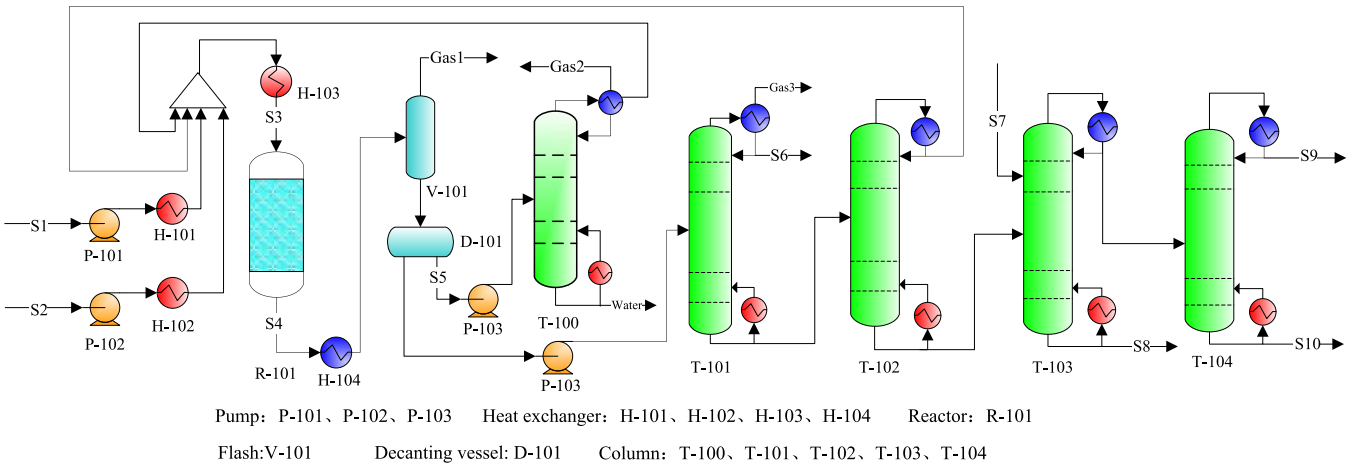

Figure 9. Process flowsheet diagram for case 1.

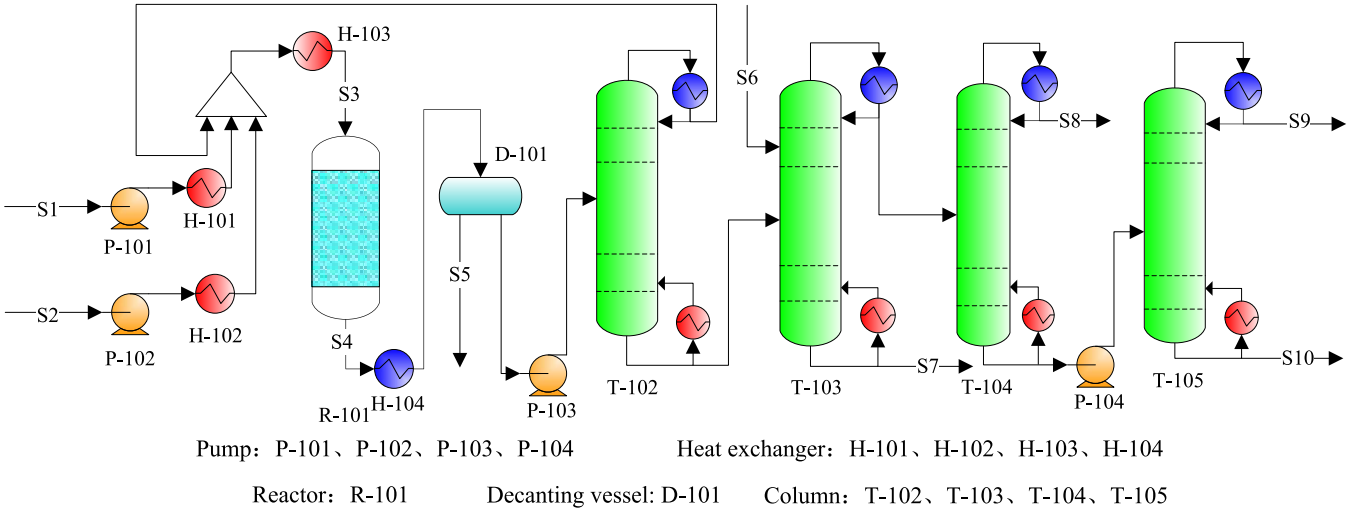

Figure 10. Process flowsheet diagram for case 2.

3. DESIGN OF SHORT PROCESSES AND OPTIMIZATION OF PX PRODUCTION

3.1. Design of the Short Process. Based on the PX selectivity sensitivity analysis, it was possible to achieve an S_{PX} of more than 99.7 wt % in the toluene methylation reactor. The subsequent product purification would avoid C8 isomer separation, which is usually carried out using adsorptive, crystallization, or reactive distillation technologies, and it also shortened the PX production process. To illustrate the shorter process, the existing PX production process, as well as our modified process, will also be explained, based on the reaction kinetics model for the two catalysts.

3.1.1. Cases 1 and 2: Ashraf's Process for Catalysts A and B. An existing PX production process proposed by Ashraf et al.,[23] was used as case 1 (Figure 9). Ashraf's process was based on a fixed-bed toluene methylation reactor using catalyst A. As shown in Figure 9, the two feeds (toluene and methanol at atmospheric pressure and ambient temperature) were first preheated and then mixed with the recycled methanol and toluene stream. After heating to the reaction temperature, the reactor feed (S3) conditions were set to a certain feed ratio, temperature, and pressure using the Aspen Plus design specifications tool. Next, the reactor product stream was cooled for flash separation to obtain light compounds, such as gaseous hydrocarbons (gas 1). The liquid stream was fed into a decanter vessel (D-101) to separate the water and aromatics phases, and the water-rich phase (S5) was sent to the distillation column (T-100) for methanol recovery and recycling. As the aromatic rich phase was pumped for benzene separation (T-101) and toluene recovery (T-102), the reactive distillation of the xylene isomers (T-103) and PX separation (T-104) were performed to obtain a PX product with a purity of 99.7% (S10). Typically, di-tert-butyl-benzene (DTBB) or tert-butyl-benzene (TBB) are introduced into T-103 to selectively react with m-xylene to generate tert-butyl meta-xylene (TBMX) and benzene. This reactive distillation process was used to separate PX from its isomers, as this process was more economically viable compared to adsorption and crystallization, as the mixed xylene bottom stream of T-102 was 97.5 wt % PX.[23]

For cCase 1, the operation parameters that affected the toluene methylation reactor were improved to achieve high PX selectivity. Using the optimization tool in Aspen Plus, the maximum PX selectivity was set as the objective optimization function and 40.0% methanol loss as the constraint condition for optimization during the reaction process (as shown in formula 1). The optimization results indicated that PX selectivity increased from 58.0 to 97.7%.

https://doi.org/10.1021/acsomega.1c05817
ACS Omega 2022, 7, 1211−1222

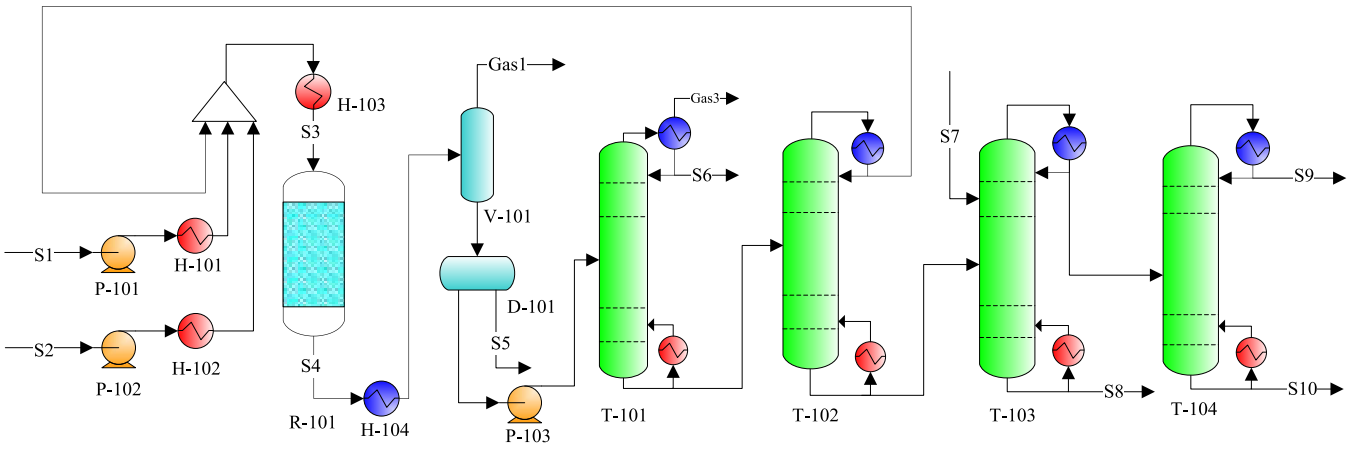

Figure 11. Process flowsheet diagram for case 3.

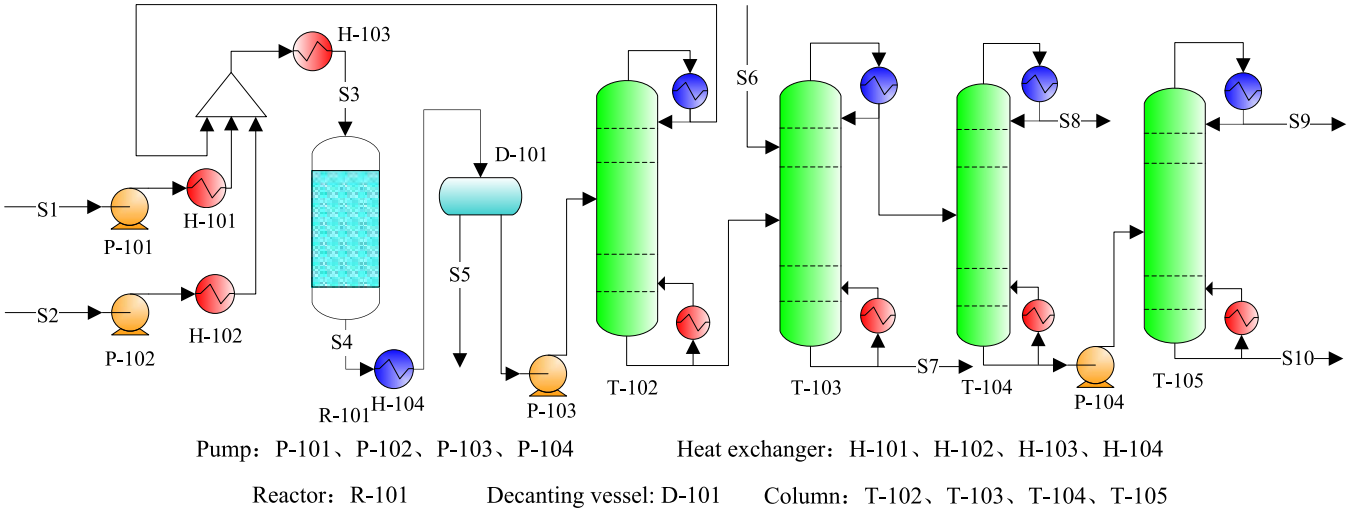

Figure 12. Process flowsheet diagram for case 4.

$$\text{objective}: \quad \max\ S_{PX} = \frac{F_{\mathrm{PX}}^{\mathrm{out}}}{\left(F_{\mathrm{MX}}^{\mathrm{out}} + F_{\mathrm{PX}}^{\mathrm{out}} + F_{\mathrm{OX}}^{\mathrm{out}}\right)}$$

$$\text{objective constraint:}\ X_{\mathrm{M}} = \frac{F_{\mathrm{M}}^{\mathrm{in}} - F_{\mathrm{M}}^{\mathrm{out}}}{F_{\mathrm{M}}^{\mathrm{in}}} \geq 40.0\ \%$$

$$\text{variables:}\ \ 2.0 \leq m \leq 8.0 \qquad (2)$$

$$420.0 \leq T \leq 550.0\ ^{\circ}\mathrm{C}$$

$$2.0 \leq P \leq 5.0\ \mathrm{kPa}$$

Note: X_i presents the conversion for component i.

Once the reaction stage in case 1 uses the reaction kinetics model for catalyst B, the process flow should be modified due to the difference of the reactor effluent, which was denoted as case 2 and is shown in Figure 10. This process had the same toluene circulation and product separation systems. Thus, the goal of case 2 was to optimize the S_{PX} by limiting the minimum conversion of methanol according to Ashraf's process. The optimized reaction process conditions for case 2 were consistent with case 1.

3.1.2. Cases 3 and 4: Liu's Process Using Catalysts A and B. An existing PX production process proposed by Liu et al.[6] was used for case 3 (Figure 11), which eliminated the methanol recovery tower T-100 and recycling system in Figure 9. In case 3 (Liu's process), the process optimized the methanol conversion rate to over 98.0% during the methylation reaction by setting the relevant constraints (as shown in formula 3).

$$\text{objective}: \quad \max\ X_{\mathrm{M}} = \frac{F_{\mathrm{M}}^{\mathrm{in}} - F_{\mathrm{M}}^{\mathrm{out}}}{F_{\mathrm{M}}^{\mathrm{in}}}$$

$$\text{objective constraint:}$$

$$S_{PX} = \frac{F_{PX}^{out}}{\left(F_{MX}^{out} + F_{PX}^{out} + F_{OX}^{out}\right)} \geq 90.0\ \%$$

$$X_T = \frac{F_T^{in} - F_T^{out}}{F_T^{in}} \geq 23.0\ \% \qquad (3)$$

$$F_{\mathrm{PX}}^{\mathrm{out}} \geq 187.00\ \mathrm{kmol \cdot h^{-1}}$$

$$\text{variables:}\ \ 2.0 \leq m \leq 8.0$$

$$420.0 \leq T \leq 550.0\ ^{\circ}\mathrm{C}$$

$$200.0 \leq P \leq 500.0\ \mathrm{kPa}$$

Note: X_i presents the conversion for component i.

Based on case 3 from Liu's process, a new process flow was also established and optimized, denoted as case 4 (Figure 12), which used and matched the reaction kinetics model for catalyst B. In addition, case 4 was expected to optimize the conversion of methanol by limiting the minimum S_{PX}, according to Liu's

https://doi.org/10.1021/acsomega.1c05817
ACS Omega 2022, 7, 1211−1222

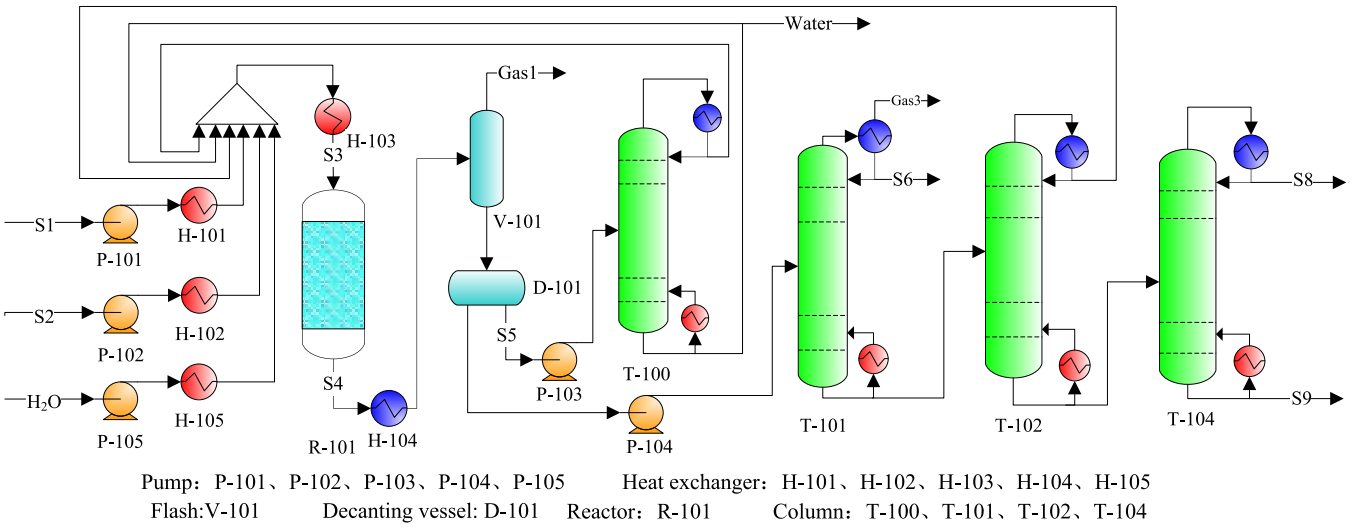

Figure 13. Process flowsheet diagram for case 5.

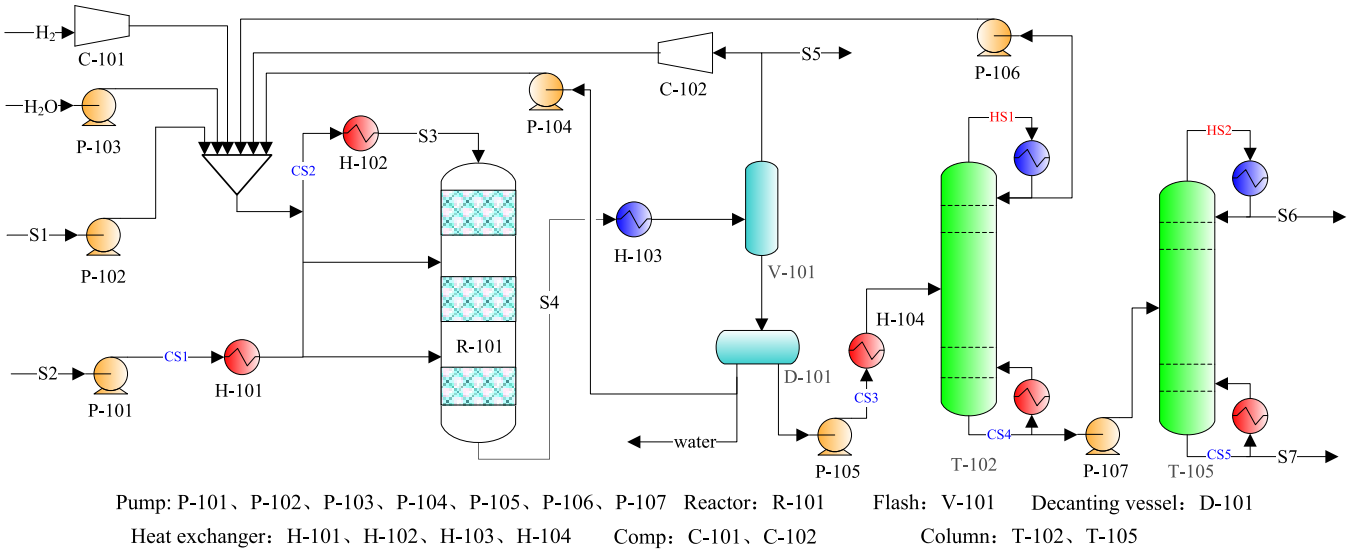

Figure 14. Short process for the PX production for case 6.

process. Thus, the optimization conditions were consistent with case 3.

Because of the relatively higher methanol conversion and without the production of benzene byproducts for catalyst B (Si−Mg−P−La/ZSM-5), case 4 included T-105 trimethylbenzene byproducts but excluded the benzene separation tower (T-101). In addition, the methanol recovery tower (T-100) was eliminated, as the unreacted methanol could be recycled with the toluene recycling system.

3.1.3. Cases 5 and 6: Short Processes Using Catalysts A and B. Once an S_{PX} of 99.7% was achieved in the methylation reactor, the reactive distillation tower (T-103) shown in Figure 9 was removed. To enhance PX selectivity, a H_2O diluent was introduced to reduce the contact time in R-101. However, when methanol conversion decreased, the methanol recovery tower (T-100) and recycling system were retained. This process is shown in Figure 13 as case 5.

When pursuing high S_{PX}, toluene conversion (X_T) will decrease significantly. Therefore, to balance the conversion rate and PX selectivity, we set the methanol conversion rate and PX selectivity as the constraints to optimize and maximize the toluene conversion rate during the reaction process (as shown in eq 3).

$$\text{objective}: \quad \max X_T = \frac{F_T^{in} - F_T^{out}}{F_T^{in}}$$

objective constraint:

$$S_{PX} = \frac{F_{PX}^{out}}{\left(F_{MX}^{out} + F_{PX}^{out} + F_{OX}^{out}\right)} \geq 99.7\ \%$$

$$X_M = \frac{F_M^{in} - F_M^{out}}{F_M^{in}} \geq 99.0\ \%$$

$$F_{PX}^{out} \geq 184.0\ \text{kmol}\cdot\text{h}^{-1}$$

variables:

$$2.0 \leq m \leq 8.0 \qquad (4)$$

$$420.0 \leq T \leq 550.0\ ^\circ\text{C}$$

$$200.0 \leq P \leq 500.0\ \text{kPa}$$

$$0.2 \leq w \leq 10.0$$

$$0.2 \leq n \leq 8.0$$

$$0.2 \leq n' \leq 8.0$$

Note: X_i presents the conversion for component i.

However, by optimizing the feed ratio, diluent amount, temperature, and pressure, the S_{PX} in the methylation reactor

https://doi.org/10.1021/acsomega.1c05817
ACS Omega 2022, 7, 1211−1222

Table 3. Optimal Operating Conditions for the Reactor

process	T, °C	P, kPa	W_{cat}/F_T, g·h·mol^{-1}	F_T/F_M	S_{PX}, %	X_T, %	X_M, %
Case 1[23]	400.0	300.0	2.50	2.00	97.70	23.00	65.50
Case 2	420.0	400.0	2.20	4.60	96.80	20.90	99.90
Case 3[6]	442.5	400.0	3.40	1.90	92.00	28.20	98.00
Case 4	442.5	400.0	2.20	4.60	96.40	20.70	99.90
Case 5	442.5	400.0	0.95	6.43	99.26	5.37	41.89
Case 6	470.0	350.0	1.20	8.10	99.71	12.00	92.12

Table 4. Total Material Balance of the Six Cases

	input, kmol·h^{-1}				output, kmol·h^{-1}									
process	T	M	H_2O	H_2	T	M	GH	B	OX	PX	MX	TMB	H_2O	H_2
Case 1[23]	215.20	393.60	0.00	0.00	16.10	62.39	75.10	8.32	2.49	187.41	0.02	0.00	330.61	0.00
Case 2	193.00	197.00	0.00	0.00	1.48	0.00	0.00	3.07	3.17	180.14	0.14	5.48	197.00	0.00
Case 3[6]	215.20	393.00	0.00	0.00	3.51	8.40	94.19	13.7	8.11	187.69	0.20	0.00	384.6	0.00
Case 4	194.00	197.00	0.00	0.00	2.10	0.00	0.00	3.23	3.58	180.15	0.18	5.10	197.00	0.00
Case 5	207.00	257.00	2000	0.00	14.97	24.32	32.28	11.96	0.66	178.72	0.66	0.00	2232.67	0.00
Case 6	185.50	187.00	2371	90.00	2.35	0.02	0.01	0.00	0.24	178.83	0.27	3.82	2555.10	90.0

surpassed 99.7% for catalyst B, and the reactor effluent could only be purified through the two conventional distillation towers. T-102 was used for the recovery of toluene and trace methanol, while T-105 was used to separate xylene and trimethylbenzene. This short PX production process is shown and labeled as case 6 in Figure 14.

To create a fair comparison, the optimized reaction processing conditions in case 6 were the same as case 5 for the short process. To ensure selectivity intensification, both H_2O and H_2 were fed as diluents and methanol input into the reactor (R-101) in three stages. These strategies reduced the contact time and methanol partial pressure, as well as increased the ratio of toluene to methanol, which increased the S_{PX} to more than 99.7%. Thus, the xylene distillate of T-105 was the PX product.

3.2. Optimal Processing Conditions. The six cases were used to produce ~179 kmol·h^{-1} of PX product with a purity of 99.7 wt %. Afterward, the optimal operating conditions in the methylation reactor were adjusted using the sequential quadratic programming (SQP) optimization method in Aspen Plus. The reactor optimized results for the six cases are shown in Table 3, and the results of the import and export material balance of the whole process are shown in Table 4. The detailed calculated results for the processing streams, for all six cases, are shown in Tables S1−S6.

4. RESULTS AND DISCUSSION FOR THE SHORT PROCESS

4.1. Effective Utilization of Raw Materials. Table 5 shows the utilization of the raw materials for the six cases. For comparison, the effective utilization of toluene or methanol (E_i) was introduced and defined as follows

$$E_i = \frac{F_{PX}^{product}}{F_{feed,i}} \times 100\% \quad (5)$$

where $F_{PX}^{product}$ is the molar flow of PX product for each case and $F_{feed,i}$ is the molar flow of toluene or methanol. Thus, the effective utilization represents the conversion efficiency of the raw materials in the target product.

Table 5. Effective Utilization of Raw Materials

	feed, kmol·h^{-1}				
process	toluene	methanol	PX product, kmol·h^{-1}	E_T, %	E_M, %
Case 1[23]	215.24	393.65	178.59	82.97	45.36
Case 2	193.00	197.00	178.34	92.40	90.52
Case 3[6]	215.24	393.00	178.37	82.87	45.38
Case 4	194.00	197.00	178.87	92.67	90.79
Case 5	207.00	257.00	178.54	86.25	69.47
Case 6	185.50	187.00	178.59	96.27	95.50

Table 6. Energy Consumption Results of Six Cases

processes		Case 1	Case 2	Case 3	Case 4	Case 5	Case 6
utility load, MW	heat	69.30	39.28	54.50	41.80	62.10	35.70
	cold	66.60	41.87	52.80	44.50	49.60	38.30

As shown in Table 5, the short process using catalyst A (Mg/ZSM-5) in case 5 had an effective utilization rate of 86.25 and 69.47% for toluene and methanol, respectively. Both of these values were higher than cases 1 and 3. Case 5 only required 257.0 kmol·h^{-1} of methanol feed, which was much lower than the 393.0 kmol·h^{-1} required for cases 1 and 3. Thus, PX selectivity intensification inhibited the methanol dehydration reaction but increased the atomic economy of the methylation system. Similarly, the short process using catalyst B (Si−Mg−P−La/ZSM-5) in case 6 exhibited the highest effective utilization rates for toluene and methanol among all of the cases using catalyst B. For the effective utilization of toluene and methanol, we obtained values of 96.27 and 95.50%, and these values were the highest among the six cases. In addition, both kinetic models did not consider the related deactivation problems of carbon deposition,[23−25] and carbon deposition was expected in cases 1−4 due to the very little excess oxygen and hydrogen in the feed, while the diluents of H_2O and H_2 would reduce the probability of methanol to olefins and carbon accumulation.[4] Therefore, the short process would have greater advantages since they already have better feed utilization and the atomic economy than the existing processes in addition to simplifying the overall process.

4.2. Energy Consumption Analysis. To compare the energy consumption, heat integration was conducted for the six cases based on the pinch analysis method. A heat exchanger

https://doi.org/10.1021/acsomega.1c05817
ACS Omega 2022, 7, 1211−1222

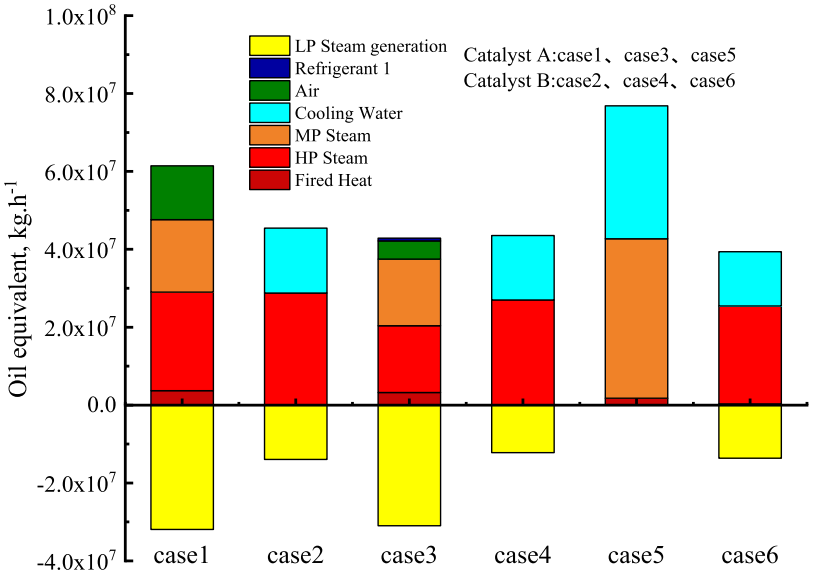

Figure 15. Breakdown of total energy consumption of the six cases measured by oil equivalent.

Table 7. Calculation Formulae and Data for Economic Analysis[a]

TCI, k$		TOC, k$·year^{-1}	
columns shell, k$	$22688.6 \times D^{1.066} \times H^{0.802}$	fired heat	17.1×10^{-3} $·kW^{-1}
columns tray, k$	$1426.0 \times D^{1.55} \times H$	cooling water	3.6×10^{-4} $·kW^{-1}
H, m	$H = \frac{N}{eT} \times 0.6096$	electricity	0.132 $·kW^{-1}·h^{-1}
heaters, $	$9367.8 \times A^{0.65}$	HP steam	35.6×10^{-3} $·kW^{-1}
A, m^2	$A = \frac{Q}{u \times \Delta T}$	MP steam	29.6×10^{-3} $·kW^{-1}
TAC, k$·year^{-1}	$TAC = \frac{TCI}{3} + TOC$	LP steam	28.0×10^{-3} $·kW^{-1}

[a]Note: D is the column diameter (m), N is the number of trays, e_T is the tray efficiency of 0.85, Q is the cooling or heating energy consumption (kW), and u is the heat-transfer coefficient (kW·°C^{-1}·m^{-2}).

Table 8. Economic Comparative Results for the Six Cases

process	TCI, k$	TOC, k$·year^{-1}	TAC, k$·year^{-1}
Case 1[23]	17 417.80	14 290.50	20 096.40
Case 2	17 020.00	10 789.72	16 463.15
Case 3[6]	14 698.10	10 854.60	15 753.90
Case 4	16 712.00	11 236.33	16 807.09
Case 5	15 410.00	13 129.00	18 265.00
Case 6	14 046.00	9166.10	13 848.10

network (HEN) was created using the Aspen energy analyzer. The minimum temperature difference (ΔT_{min}) was assumed to be 10 °C, according to Liu's strategy for cases 1 and 3.[6] The heat integration information is provided in the Supporting Information (shown in Tables S7−S12 and Figures S7−S18), including the initial hot and cold stream data and the HEN for the minimum energy requirements. The target utility energy consumption is also provided in Table 6.

As shown in Table 6, for catalyst A, the cold load of case 5 was the least, while the hot load of case 5 was less than case 1 but higher than case 3. However, the total utility energy consumption in cases 2, 4, and 6 with catalyst B was lower than that of catalyst A (cases 1, 3, and 5), which was issued by the difference in reactor production. Due to the lack of LP steam generation, the short process in case 5 required the largest amount of energy. However, the short process in case 6 also required the least amount of cooling and heating. According to GB/T 50441-2016, the utilities were expressed as the oil equivalent for different types of utilities to provide a fair comparison, and the distribution of different utilities is shown in Figure 15. The data showed that the proposed short process in case 6 required minimal heating and cooling utilities.

4.3. Technoeconomic Analysis. The total annual cost (TAC, k$·year^{-1}) was used to evaluate the economic process for all six cases. The TAC was defined according to a 3 year payback period, following the TAC calculations in ref 6, which included the total capital investment (TCI) and total operating cost (TOC). The calculations, formulae, and economic data for equipment and utilities are provided in Table 7. The calculations were based on a PX product of 179.0 kmol·h^{-1} and an annual operating time of 8000 h·year^{-1}.

The economic analysis results are shown in Table 8 and Figure 16. For the short process in case 5 using catalyst A, the annual costs were very high due to the large amount of the recirculating raw material. The short process in case 6 using catalyst B exhibited a good economic value in terms of capital investment and operating cost, and the TCI and TOC were 14 046 and 9166 k$·year^{-1}, respectively. In addition, the TAC was 13 848.1 k$·year^{-1}, which was 68.9 and 87.9% for cases 1 and 3, respectively.

5. CONCLUSIONS

In this study, a novel short process was proposed based on PX selectivity intensification of toluene methylation to minimize the high-energy consumption separation process of xylene isomers.

https://doi.org/10.1021/acsomega.1c05817
ACS Omega 2022, 7, 1211−1222

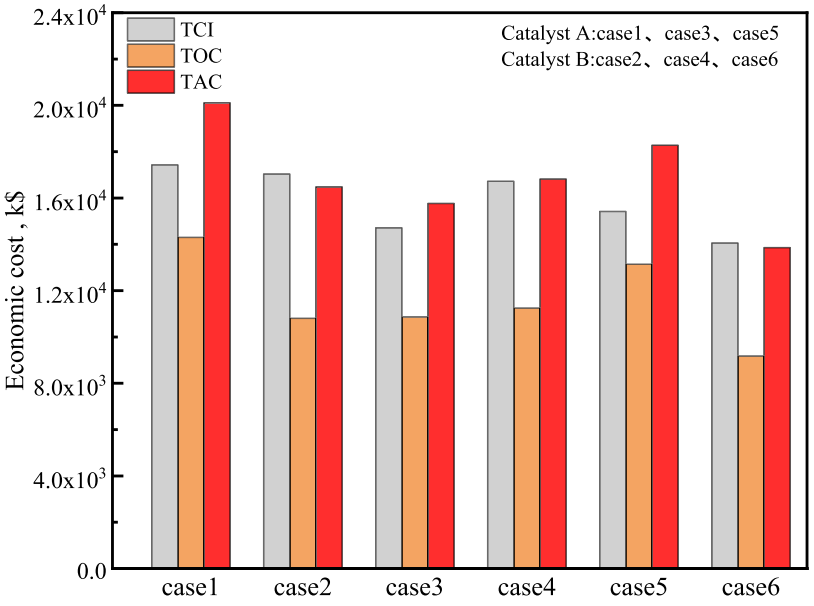

Figure 16. Economic analysis diagram of six cases.

Based on two different catalytic kinetics, we determined the influencing factors for PX selectivity intensification and constructed six cases for PX production, including a short process, to analyze raw material utilization, energy consumption, and economics. The following conclusions were drawn:

(1) To achieve selectivity intensification, we decreased the contact time according to several factors such as the feed ratio, diluents, temperature, and pressure. We then enhanced the PX selectivity of the xylene isomers to more than 99.7%.

(2) The proposed short process eliminated the separation of xylene isomers via reactive distillation, and the intensification strategy enhanced the feed utilization and atomic economy, in addition to simplifying the overall process. Specifically, the short process using catalyst Si−Mg−P−La/ZSM-5 in case 6 had the highest effective utilization rates of 96.27 and 95.50% for toluene and methanol, respectively.

(3) The proposed short process increased raw material recirculation. Because selectivity intensification still maintained many light components in the reactor effluent, such as methanol and benzene in case 5 using catalyst Mg/ZSM-5, the recirculation system significantly increased the energy consumption and TAC. However, the short process in case 6 showed a good economic value in terms of capital investment and operating costs due to the multistage reactor without benzene byproducts. The TAC was 13 848.1 k$·year^{-1}for case 6, which was 68.9 and 87.9% of the existing processes in cases 1 and 3, respectively.

■ ASSOCIATED CONTENT

Supporting Information

The Supporting Information is available free of charge at https://pubs.acs.org/doi/10.1021/acsomega.1c05817.

Detailed stream information for the six cases (Tables S1−S6), the heat integration for the initial hot and cold stream data information (Tables S7−S12), and the GCC and HEN for the minimum energy requirements (Figures S7−S18) (PDF)

■ AUTHOR INFORMATION

Corresponding Authors

Guixian Li − *School of Petrochemical Engineering, Lanzhou University of Technology, Lanzhou 730050 Gansu, China; Key Laboratory of Low Carbon Energy and Chemical Engineering of Gansu Province, Lanzhou 730050 Gansu, China*; Email: lgxwyf@163.com

Yong Yang − *School of Petrochemical Engineering, Lanzhou University of Technology, Lanzhou 730050 Gansu, China; Key Laboratory of Low Carbon Energy and Chemical Engineering of Gansu Province, Lanzhou 730050 Gansu, China*; orcid.org/0000-0003-1588-6273; Email: yangy@lut.edu.cn

Authors

Dongliang Wang − *School of Petrochemical Engineering, Lanzhou University of Technology, Lanzhou 730050 Gansu, China; Key Laboratory of Low Carbon Energy and Chemical Engineering of Gansu Province, Lanzhou 730050 Gansu, China*

Junqiang Zhang − *School of Petrochemical Engineering, Lanzhou University of Technology, Lanzhou 730050 Gansu, China; Key Laboratory of Low Carbon Energy and Chemical Engineering of Gansu Province, Lanzhou 730050 Gansu, China*

Peng Dong − *School of Petrochemical Engineering, Lanzhou University of Technology, Lanzhou 730050 Gansu, China; Key Laboratory of Low Carbon Energy and Chemical Engineering of Gansu Province, Lanzhou 730050 Gansu, China*

Xueying Fan − *Automation Institute, PetroChina Lanzhou Petrochemical Company, Lanzhou 730060 Gansu, China*

Complete contact information is available at: https://pubs.acs.org/10.1021/acsomega.1c05817

Author Contributions

‖D.W. and J.Z. contributed equally to this work.

Notes

The authors declare no competing financial interest.

■ ACKNOWLEDGMENTS

The authors are grateful for the financial support from the Major Science and Technology Project of Gansu Province (No. 19ZD2GD001).

■ NOMENCLATURE

A_i pre-exponential factor, $mol\cdot(g\cdot h\cdot atm^2)^{-1}$ or $mol\cdot(g\cdot h\cdot atm)^{-1}$
k_i rate constant, $mol\cdot(g\cdot h\cdot atm^2)^{-1}$ or $mol\cdot(g\cdot h\cdot atm)^{-1}$
E_i activation energy, $kJ\cdot mol^{-1}$
T temperature, °C
P pressure, kPa
wt mass percent, %
S_{PX} *p*-xylene selectivity, %
X_T toluene conversion rate, %
X_M methanol conversion rate, %
F_T toluene molar flow rate (in: reactor inlet, out: reactor outlet), $kmol\cdot h^{-1}$
F_M methanol molar flow rate (in: reactor inlet, out: reactor outlet), $kmol\cdot h^{-1}$
F_{PX} *p*-xylene molar flow rate (out: reactor outlet), $kmol\cdot h^{-1}$
F_{MX} *m*-xylene molar flow rate (out: reactor outlet), $kmol\cdot h^{-1}$
F_{OX} *o*-xylene molar flow rate (out: reactor outlet), $kmol\cdot h^{-1}$
W_{cat} catalyst weight, kg
m F_T/F_M
n F_{H_2}/F_M or $(n' = F_{N_2}/F_M)$
w F_{H_2O}/F_M
τ contact time, s

Subscriptsand Compounds

i reaction number
H_2 hydrogen
N_2 nitrogen
C_2H_4 ethylene
B benzene
T toluene
M methanol
MX *m*-xylene
OX *o*-xylene
PX *p*-xylene
TMB trimethyl-benzene
DTBB di-*tert*-butyl-benzene
GH light gaseous hydrocarbons
TBB *tert*-butyl-benzene
TBMX *tert*-butyl *m*-xylene
H_2O water

■ REFERENCES

(1) Zhou, J.; Liu, Z.; Wang, Y.; Kong, D.; Xie, Z. Shape selective catalysis in methylation of toluene: Development, challenges and perspectives. *Front. Chem. Sci. Eng.* **2018**, *12*, 103−112.
(2) Wang, D.; Su, X.; Fan, Z.; Wen, Z.; Li, N.; Yang, Y. Recent advances for selective catalysis in benzene methylation: reactions, shape-selectivity and perspectives. *Catal. Surv. Asia* **2021**, *25*, 1−15.
(3) Chakinala, N.; Chakinala, A. G. Process design strategies to produce p-Xylene via toluene methylation: A review. *Ind. Eng. Chem. Res.* **2021**, *60*, 5331−5351.
(4) Ulyev, L. M.; Kanischev, M. V.; Chibisov, R. E.; Vasilyev, M. A. Heat integration of an industrial unit for the ethylbenzene production. *Energies* **2021**, *14*, No. 3839.
(5) Busca, G. Production of Gasolines and Monocyclic Aromatic Hydrocarbons: From Fossil Raw Materials to Green Processes. *Energies* **2021**, *14*, No. 4061.
(6) Liu, J.; Yang, R.; Wei, Sa.; Shen, W.; Rakovitis, N.; Li, J. Intensified p-Xylene production process through toluene and methanol alkylation. *Ind. Eng. Chem. Res.* **2018**, *57*, 12829−12841.
(7) Song, W.; Hou, Y.; Chen, Z.; Cai, D.; Qian, W. Process simulation of the syngas-to-aromatics processes: Technical economics aspects. *Chem. Eng. Sci.* **2020**, *212*, No. 115328.
(8) Zhang, D.; Yang, M.; Feng, X. Aromatics production from methanol and pentane: Conceptual process design, comparative energy and techno-economic analysis. *Comput. Chem. Eng.* **2019**, *126*, 178−188.
(9) Huang, X.; Wang, R.; Pan, X.; Wang, C.; Fan, M.; Zhu, Y.; Wang, Y.; Peng, J. Catalyst design strategies towards highly shape-selective HZSM-5 for para-xylene through toluene alkylation. *Green Energy Environ.* **2020**, *5*, 385−393.
(10) Niziolek, A. M.; Onel, O.; Floudas, C. A. Production of Benzene, Toluene, and Xylenes from Natural Gas via Methanol: Process Synthesis and Global Optimization. *AIChE J.* **2016**, *62*, 1531−1556.
(11) Breen, J.; Burch, R.; Kulkarni, M.; Collier, P.; Golunski, S. Enhanced para-Xylene Selectivity in the Toluene Alkylation Reaction at Ultralow Contact Time. *J. Am. Chem. Soc.* **2005**, *127*, 5020−5021.
(12) Chen, Q.; Liu, J.; Yang, B. Identifying the key steps determining the selectivity of toluene methylation with methanol over HZSM-5. *Nat. Commun.* **2021**, *12*, No. 3725.
(13) Li, J.; Ji, W.; Liu, M.; Zhao, G.; Jia, W.; Zhu, Z. New insight into the alkylation-efficiency of methanol with toluene over ZSM-5: Microporous diffusibility significantly affects reacting-pathways. *Microporous Mesoporous Mater.* **2019**, *282*, 252−259.
(14) Ghani, N. N. M.; Jalil, A. A.; Triwahyono, S.; Aziz, M. A. A.; Rahman, A. F. A.; Hamid, M. Y. S.; Izan, S. M.; Nawawi, M. G. M. Tailored mesoporosity and acidity of shape-selective fibrous silica beta zeolite for enhanced toluene co-reaction with methanol. *Chem. Eng. Sci.* **2019**, *193*, 217−229.
(15) Janardhan, H. L.; Shanbhag, G. V.; Halgeri, A. B. Shape-selective catalysis by phosphate modified ZSM-5: Generation of new acid sites with pore narrowing. *Appl. Catal., A* **2014**, *471*, 12−18.
(16) Kaeding, W.; Chu, C.; Young, L.; Butter, S. Shape-selective reactions with zeolite catalysts:II. Selective disproportionation of toluene to produce benzene and para-xylene. *J. Catal.* **1981**, *69*, 392−398.
(17) Ghiaci, M.; Abbaspur, A.; Arshadi, M.; Aghabarari, B. Internal versus external surface active sites in ZSM-5 zeolite: Part 2: Toluene alkylation with methanol and 2-propanol catalyzed by modified and unmodified H_3PO_4/ZSM-5. *Appl. Catal., A* **2007**, *316*, 32−46.
(18) Wang, C.; Zhang, L.; Huang, X.; Zhu, Y.; Li, G.; Gu, Q.; Chen, J.; Ma, L.; Li, X.; He, Q.; et al. Maximizing sinusoidal channels of HZSM-5 for high shape-selectivity to p-xylene. *Nat. Commun.* **2019**, *10*, No. 4348.
(19) Miyake, K.; Hirota, Y.; Ono, K.; Uchida, Y.; Tanaka, S.; Nishiyama, N. Direct and selective conversion of methanol to para-xylene over Zn ion doped ZSM-5/silicalite-1 core-shell zeolite catalyst. *J. Catal.* **2016**, *342*, 63−66.
(20) Li, G.; Wu, C.; Ji, D.; Dong, P.; Zhang, Y.; Yang, Y. Acidity and catalyst performance of two shape-selective HZSM-5 catalysts for alkylation of toluene with methanol. *React. Kinet. Mech. Catal.* **2020**, *129*, 963−974.
(21) Rabiu, S.; Al-Khattaf, S. Kinetics of Toluene Methylation over ZSM-5 Catalyst in a Riser Simulator. *Ind. Eng. Chem. Res.* **2008**, *47*, 39−47.
(22) Fan, Z. L.; Su, X.; Wang, D. L.; Zhang, D. Q.; Duan, R. H.; Yang, Y. Simulation of catalytic toluene alkylation with methanol in fixed-bed reactors. *Int. J. Chem. Kinet.* **2021**, *53*, 558−568.
(23) Ashraf, M. T.; Chebbi, R.; Darwish, N. A. Process of p-Xylene Production by Highly Selective Methylation of Toluene. *Ind. Eng. Chem. Res.* **2013**, *52*, 13730−13737.

https://doi.org/10.1021/acsomega.1c05817
ACS Omega 2022, 7, 1211−1222

(24) Tan, Y. T.; Zhu, R.; Zhang, X.; Tang, Y.; Zeng, Z. Kinetic Model of Toluene Alkylation with Methanol to para-Xylene. *Chem. React. Eng. Technol.* **2016**, *32*, 120−128.
(25) Palomino, J. *Alquilación de Tolueno con Metanol Mediante Catalizadores de Zeolite ZSM-5 Modificados*; Complutense University of Madrid, 1991.
(26) Sotelo, J. L.; Uguina, M. A.; Valverde, J. L.; Serrano, D. P. Deactivation Kinetics of Toluene Alkylation with Methanol over Magnesium-Modified ZSM-5. *Ind. Eng. Chem. Res.* **1993**, *32*, 2548−2554.
(27) Tang, J. Y.; Lou, B. H.; Zhang, C. L.; Ning, C. L.; Xing, H. J.; Zhu, Z. R. Shape-Selective alkylation of toluene and methanol to p-Xylene over modified HZSM-5 catalyst with high Si/Al molar ratios. *Nat. Sci.* **2013**, *52*, 23−29.
(28) Lou, B. H. Catalyst of Toluene Alkylation with Methanol to Para-Xylene, Dissertation; East China University of Science and Technology, 2014.
(29) Alabi, W.; Atanda, L.; Jermy, R.; Al-Khattaf, S. Kinetics of toluene alkylation with methanol catalyzed by pure and hybridized HZSM-5 catalysts. *Chem. Eng. J.* **2012**, *195−196*, 276−288.
(30) Tan, W.; Liu, M.; Zhao, Y.; Hou, K.; Wu, H.; Zhang, A.; Liu, H.; Wang, Y.; Song, C.; Guo, X. Para-selective methylation of toluene with methanol over nano-sized ZSM-5 catalysts: Synergistic effects of surface modifications with SiO_2, P_2O_5 and MgO. *Microporous Mesoporous Mater.* **2014**, *196*, 18−30.
(31) Wang, Y. R.; Liu, M.; Zhang, A. F.; Zuo, Y.; Ding, F. S.; Chang, Y.; Song, C. S.; Guo, X. W. Methanol Usage in Toluene Methylation over Pt Modified ZSM-5 Catalyst: Effects of Total Pressure and Carrier Gas. *Ind. Eng. Chem. Res.* **2017**, *56*, 4709−4717.

https://doi.org/10.1021/acsomega.1c05817
ACS Omega 2022, 7, 1211−1222